Journal of Geophysical Research: Solid Earth

Supporting Information for

A New Madrid Seismic Zone Fault System Model from Relative Event Locations and Application of Optimal Anisotropic Dynamic Clustering

Yixin Zhang[1], Oluwaseun Fadugba[1], Christine Powell[1], Stephen Horton[1], and Charles A. Langston[1]

[1]Center for Earthquake Research and Information, The University of Memphis, Memphis, TN

Contents of this file

Introduction

The supporting information provides details on performing event relocations with catalog data only, cross correlation data only, and the improvement in event locations when both datasets are used. A comparison between the original event locations and the relocations is given as well as the reduction in location errors produced by relocation. The OADC analyses used to select fault planes for the North and the Axial Parts of the NMSZ are presented. Fault parameters for all 31 modeled fault planes are listed in Table S1. Finally, the improvement in locations over the model obtained in the prior hypoDD study by Dunn et al., (2010) is indicated.

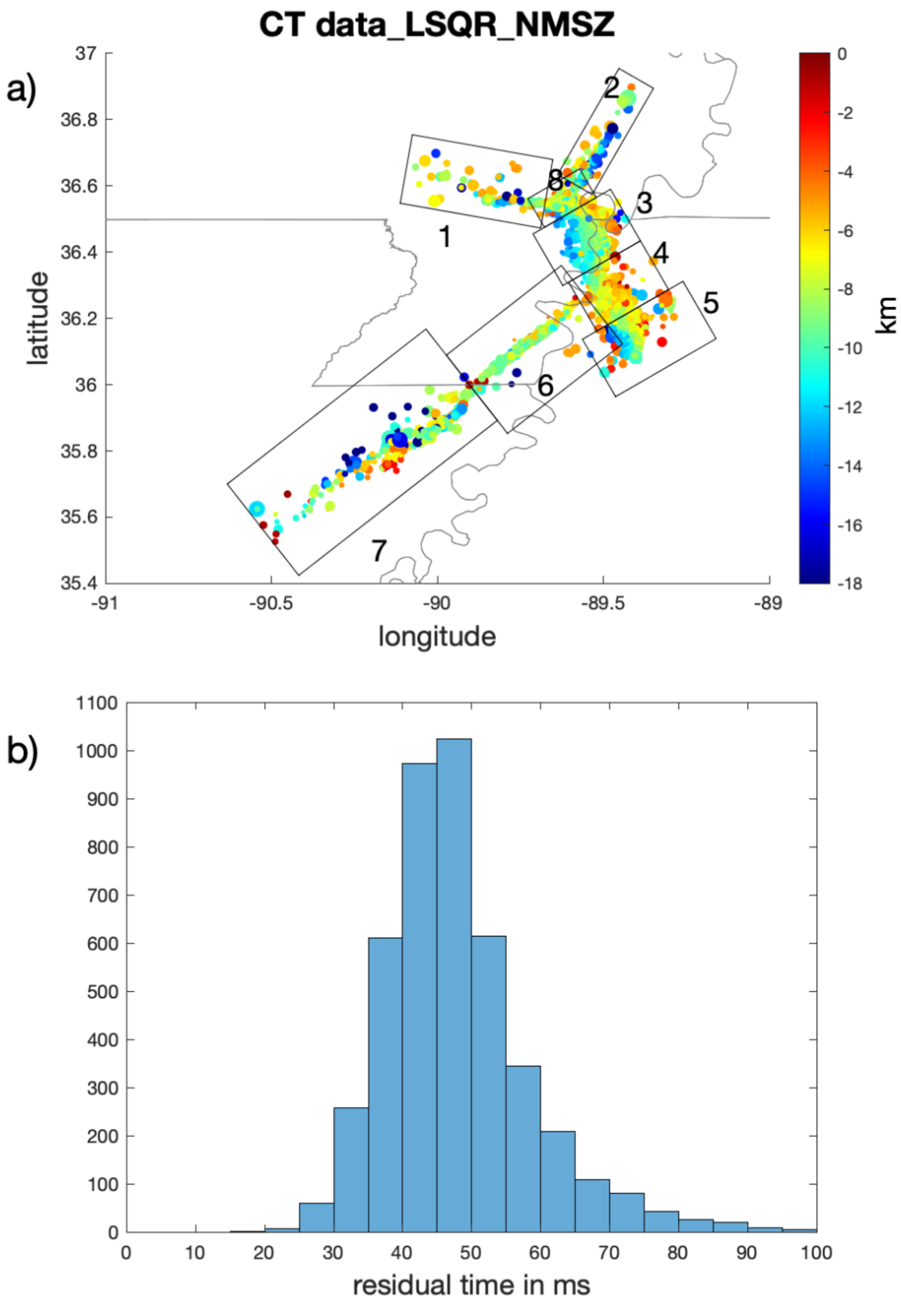

Figure S1. a) NMSZ event locations determined using HypoDD_LSQR using only catalog data. Circles represent earthquakes; the size of circles is proportional to the earthquake magnitude, **ranging from 0.1 to 3.9**. The color scale shows the hypocenter depth. b) Histogram of the residual times for the 4422 events.

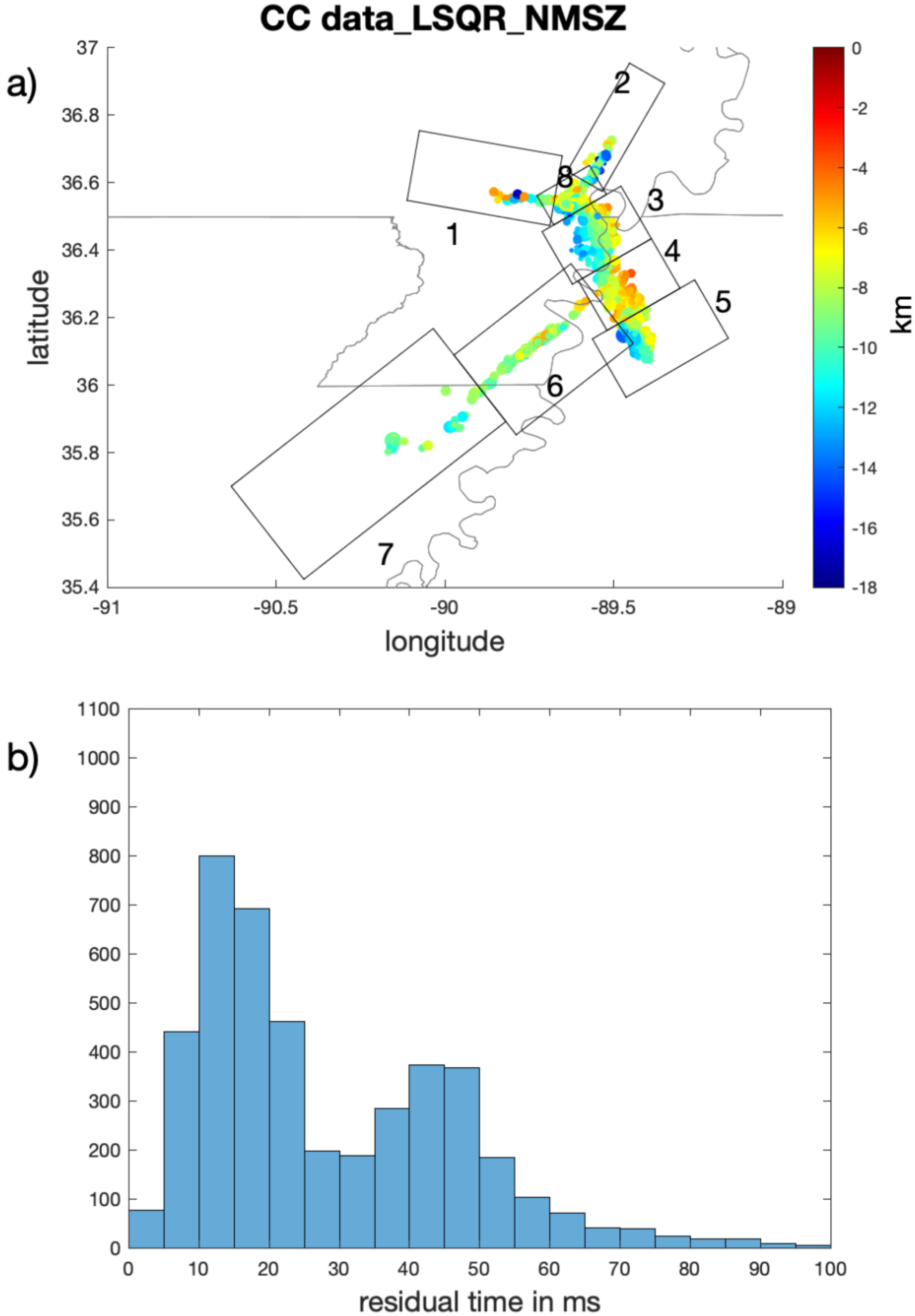

Figure S2. a) NMSZ event locations determined using HypoDD_LSQR using only cross-correlation data. Circles represent earthquakes; the size of circles is proportional to the earthquake magnitude, **ranging from 0.1 to 3.9**. The color scale shows the hypocenter depth. b) Histogram of the residual times for the 2647 events.

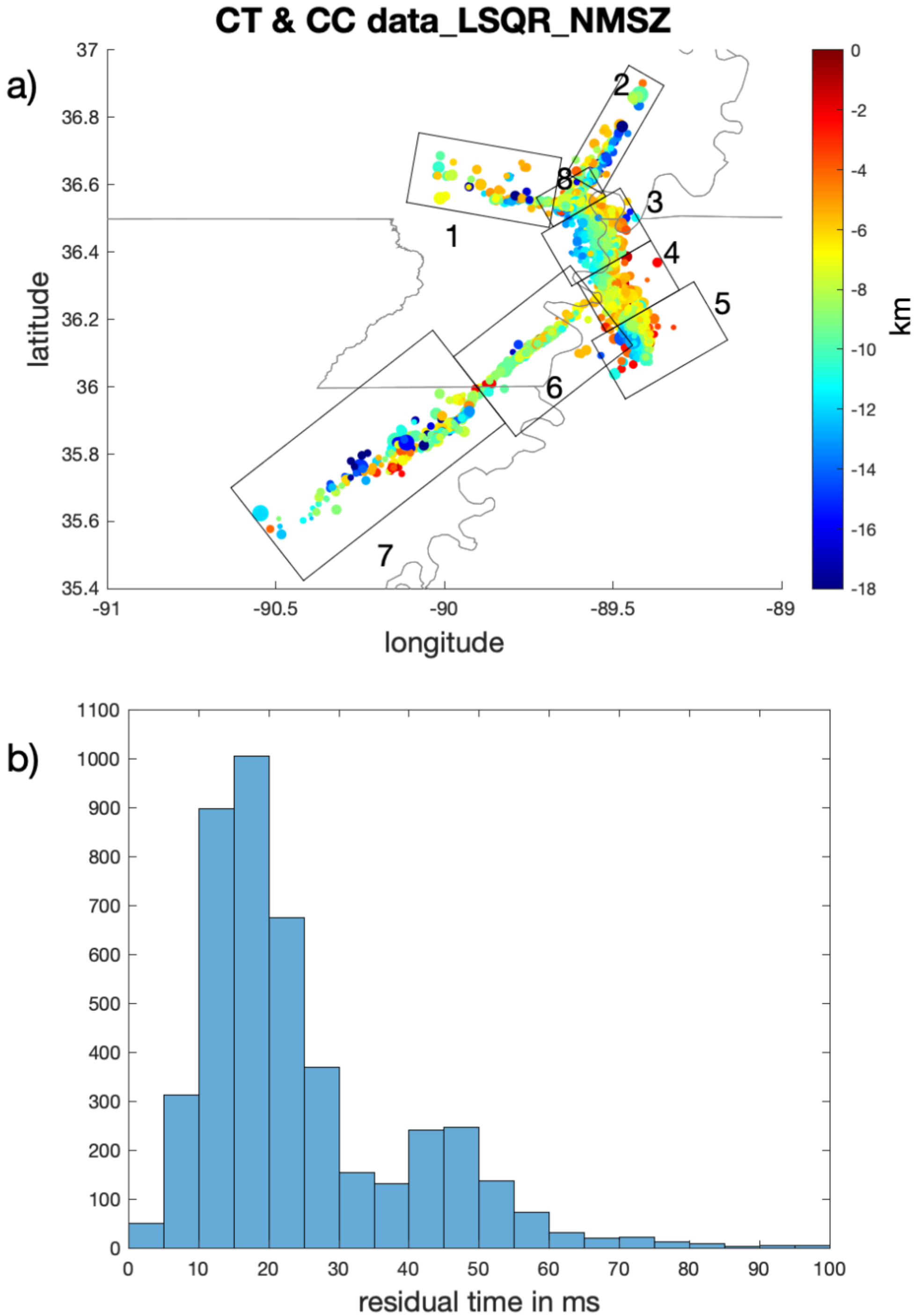

Figure S3. a) NMSZ event locations determined using HypoDD_LSQR using both catalog and cross-correlation data. Circles represent earthquakes; the size of circles is proportional to the earthquake magnitude, ranging from 0.1 to 3.9. The color scale shows the hypocenter depth. b) Histogram of the residual times for the 4032 events.

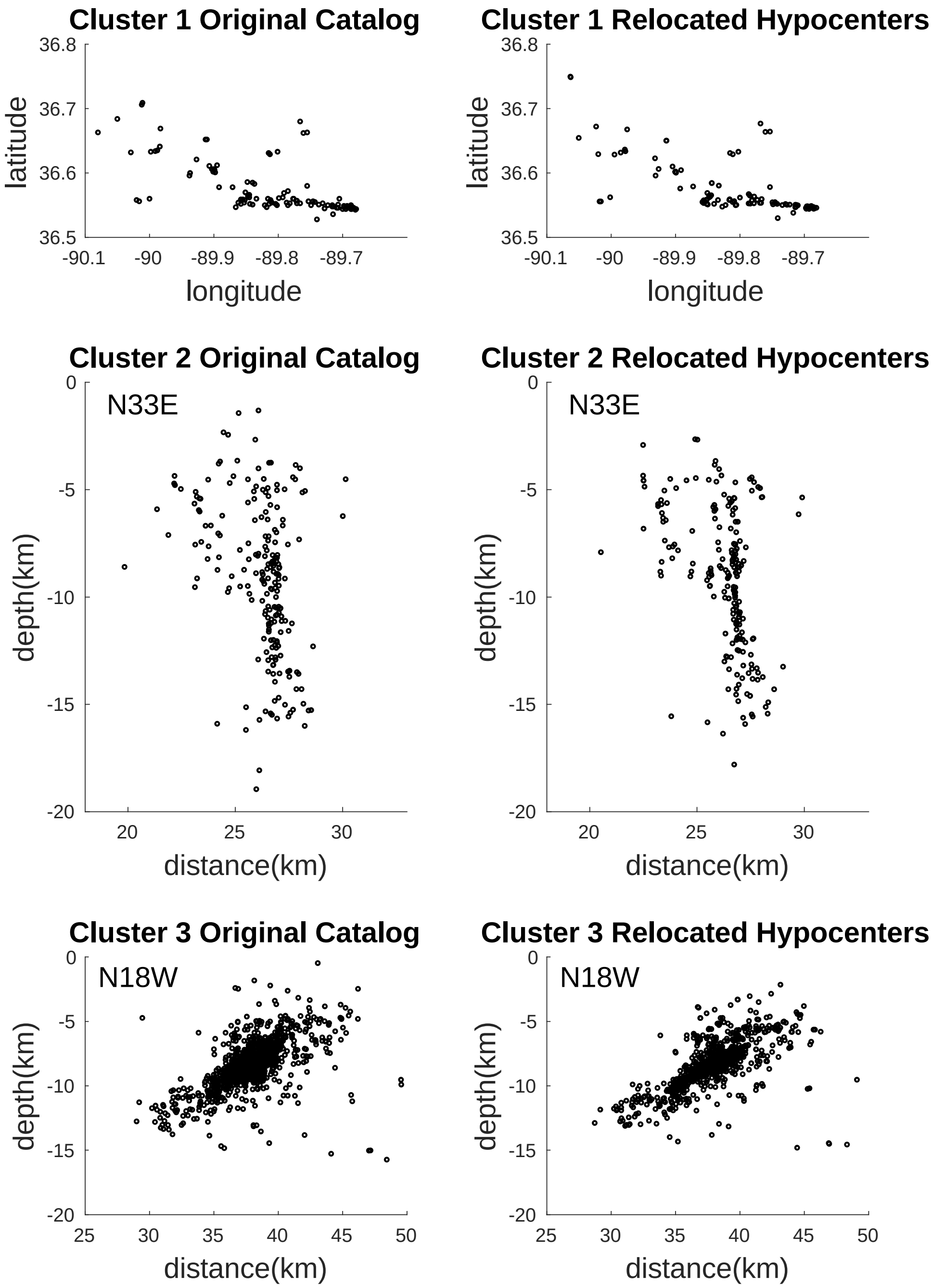

Figure S4. Comparison between the original and relocated catalog hypocenters for the clusters shown in Figure 2. For each cluster, we use the same view angle as in Dunn et al., (2010). We also use a similar way of partitioning clusters, except we separate the RF area into 3 clusters and Dunn et al. (2010) separate the area into northern and southern segments. Cluster 1 shown in map view. All other clusters shown in cross section. Cross section orientation indicated.

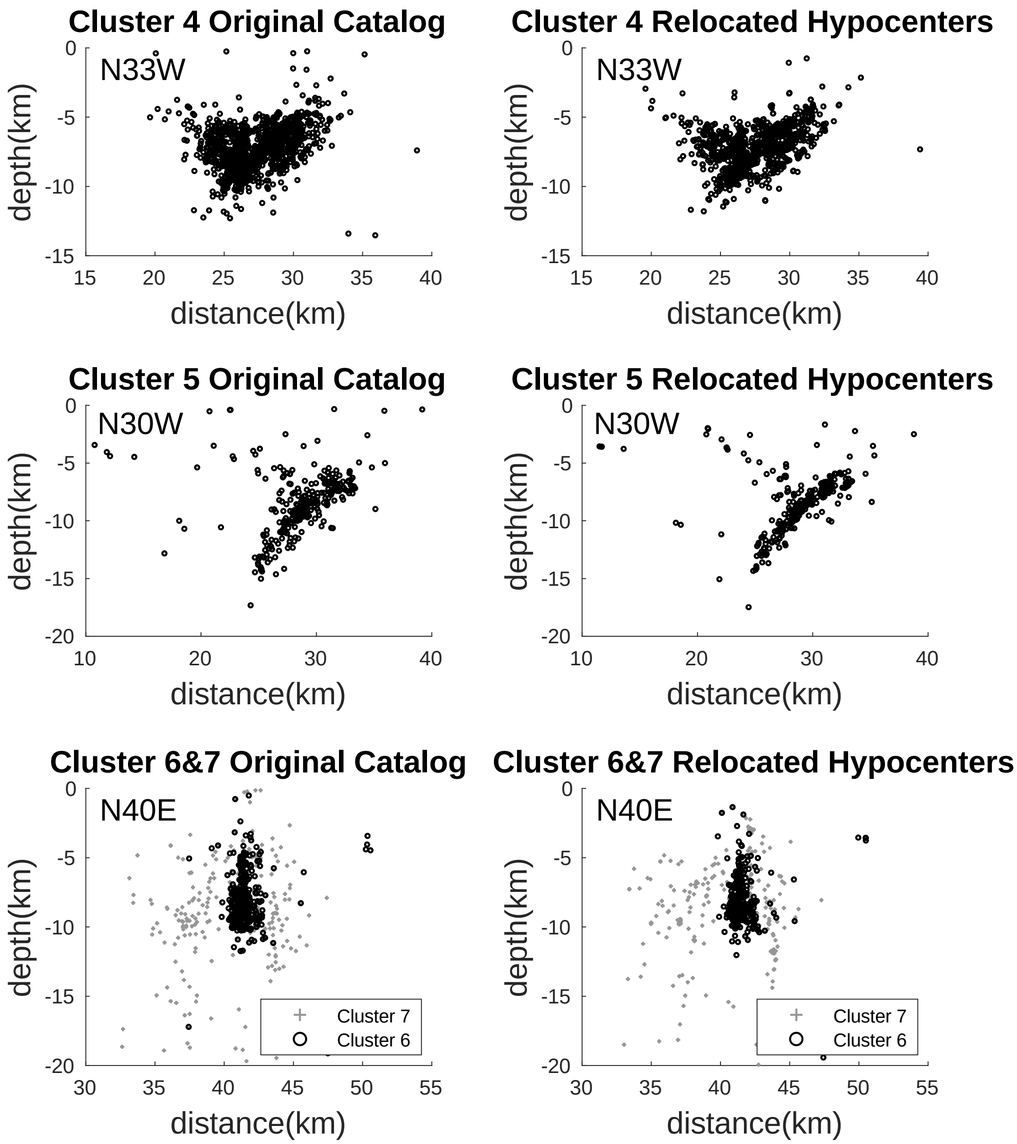

Figure S4. Continued.

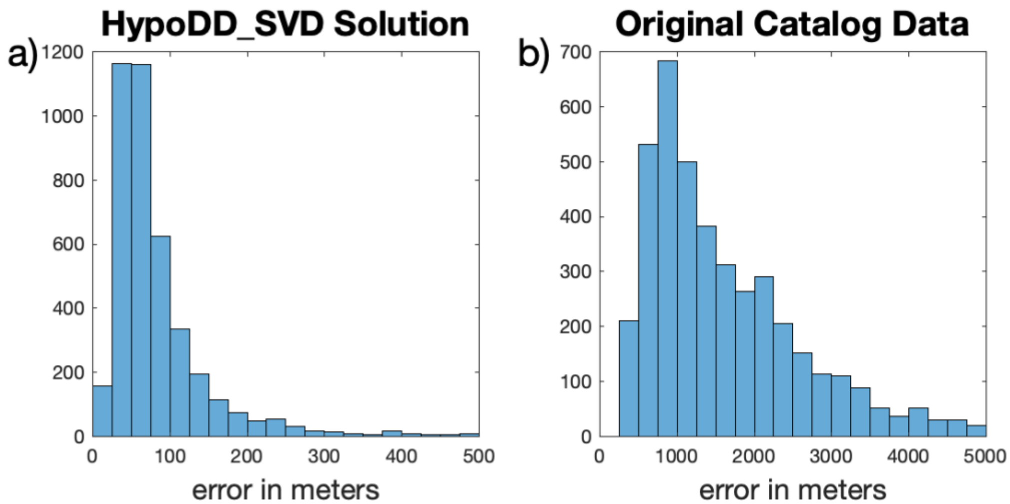

Figure S5. Histograms of earthquake location errors. a) our solution errors in meters. Most events have an error less than 150 meters. b) original catalog data errors; errors are larger than 250 meters.

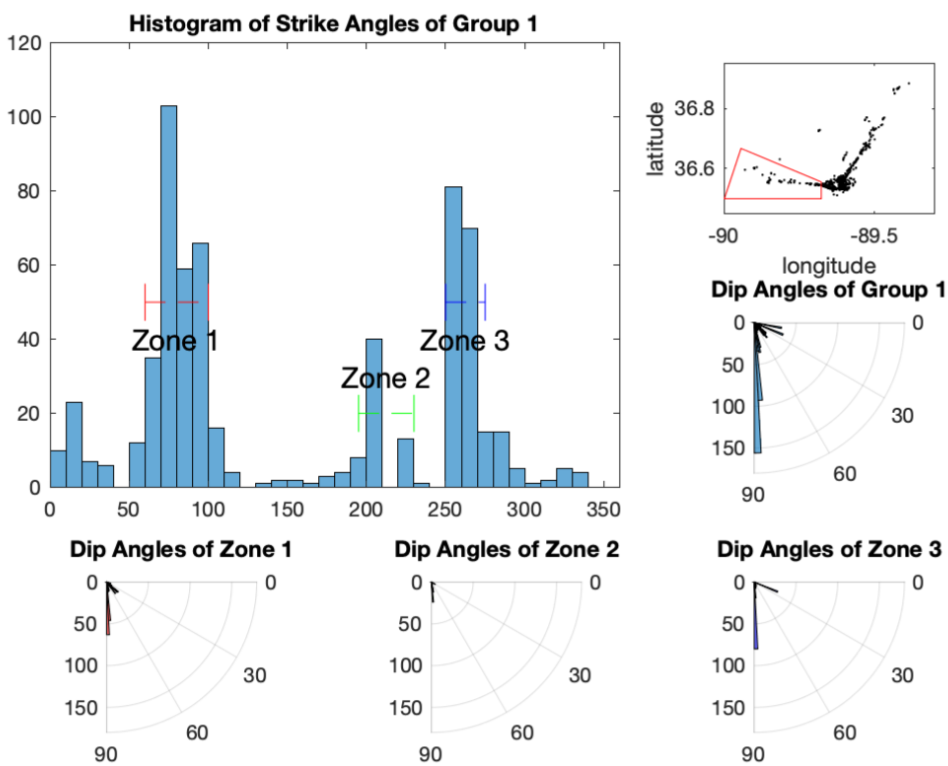

Figure S6. OADC analysis for NP group 1 (upper right). Three zones are labeled with bin values over 40. The dashed lines indicate the strike range for each zone. Rose diagrams are determined for each zone. Fault parameters for these zones are given in Table S1. No zones are used in the final fault model.

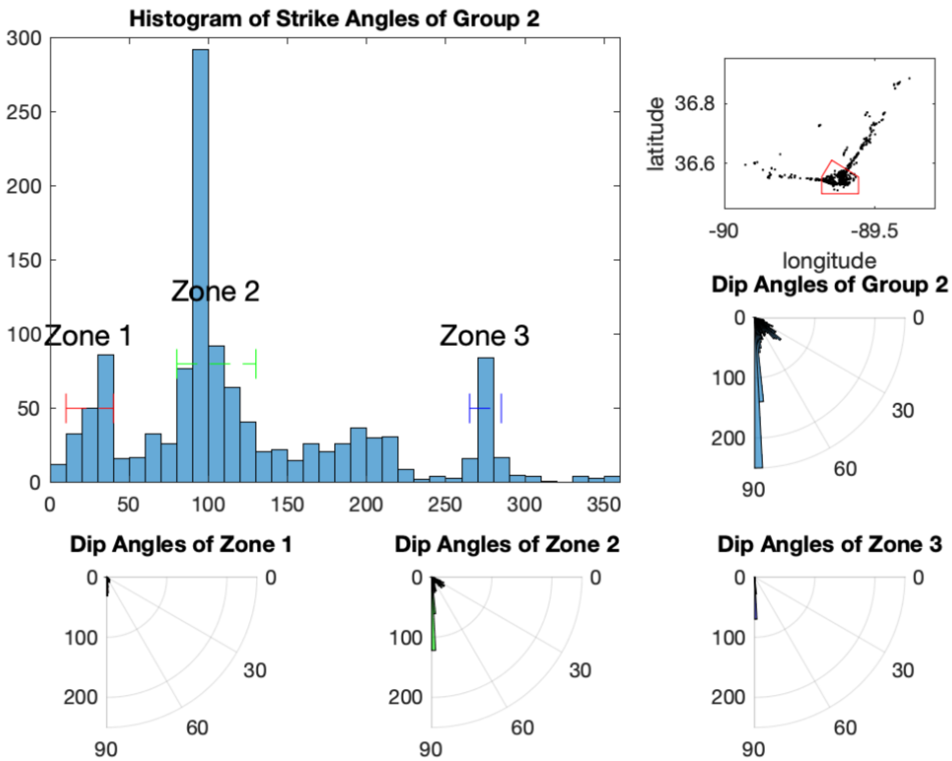

Figure S7. OADC analysis for NP group 2 (upper right). Three zones are labeled with bin values over 40. The dashed lines indicate the strike range for each zone. Rose diagrams are determined for each zone. Fault parameters for these zones are given in Table S1. Only zone 2 are used in the final model.

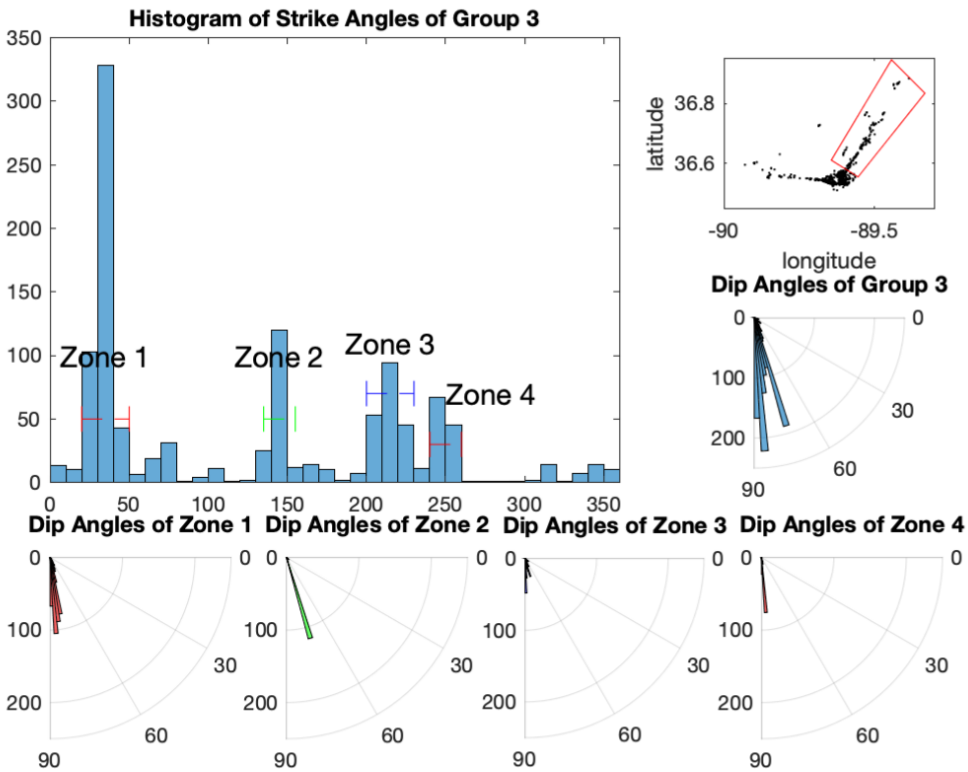

Figure S8. OADC analysis for NP group 3 (upper right). Four zones are labeled with bin values over 40. The dashed lines indicate the strike range for each zone. Rose diagrams are determined for each zone. Fault parameters for these zones are given in Table S1. Only zone 1 are used in the final model.

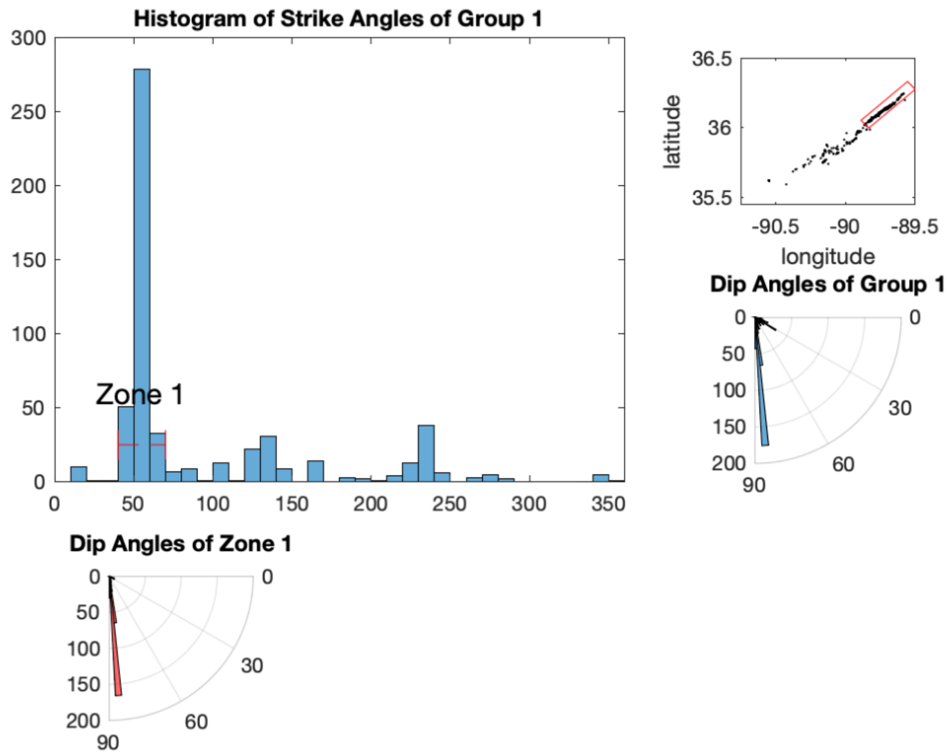

Figure S9. OADC analysis for AFP group 1 (upper right). Only one zone is labeled with bin value over 40. The dashed line indicates the strike range for the zone. Rose diagram is determined. Fault parameters for this zone are given in Table S1. The zone is used in the final model.

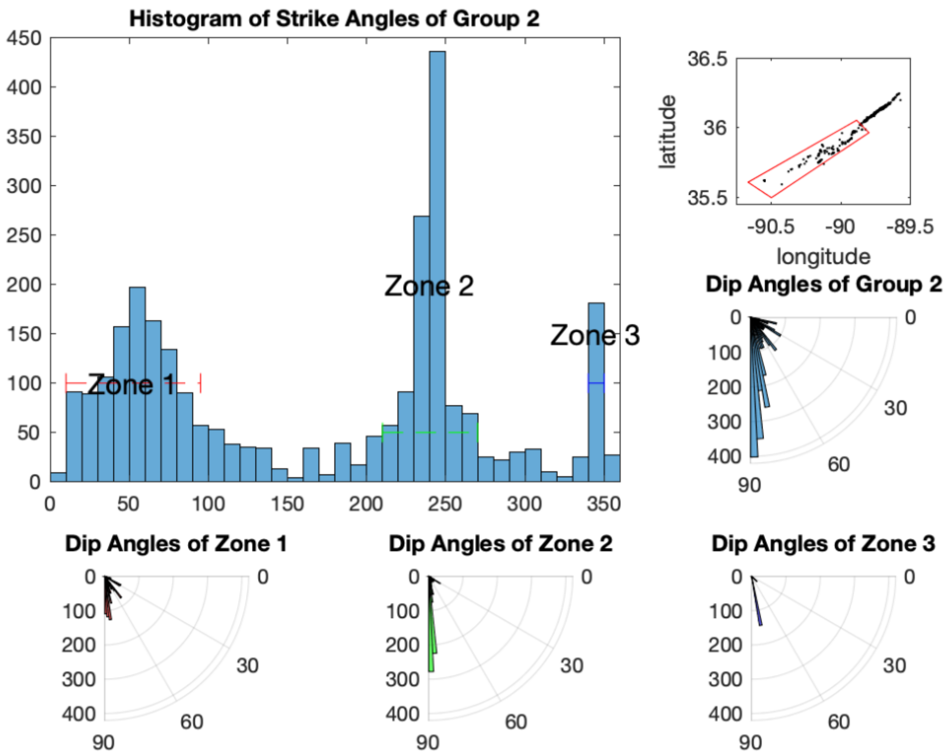

Figure S10. OADC analysis for AFP group 2 (upper right). Three zones are labeled with bin values over 40. The dashed lines indicate the strike range for each zone. Rose diagrams are determined for each zone. Fault parameters for these zones are given in Table S1. Zones 1 and 2 are used in the final mode.

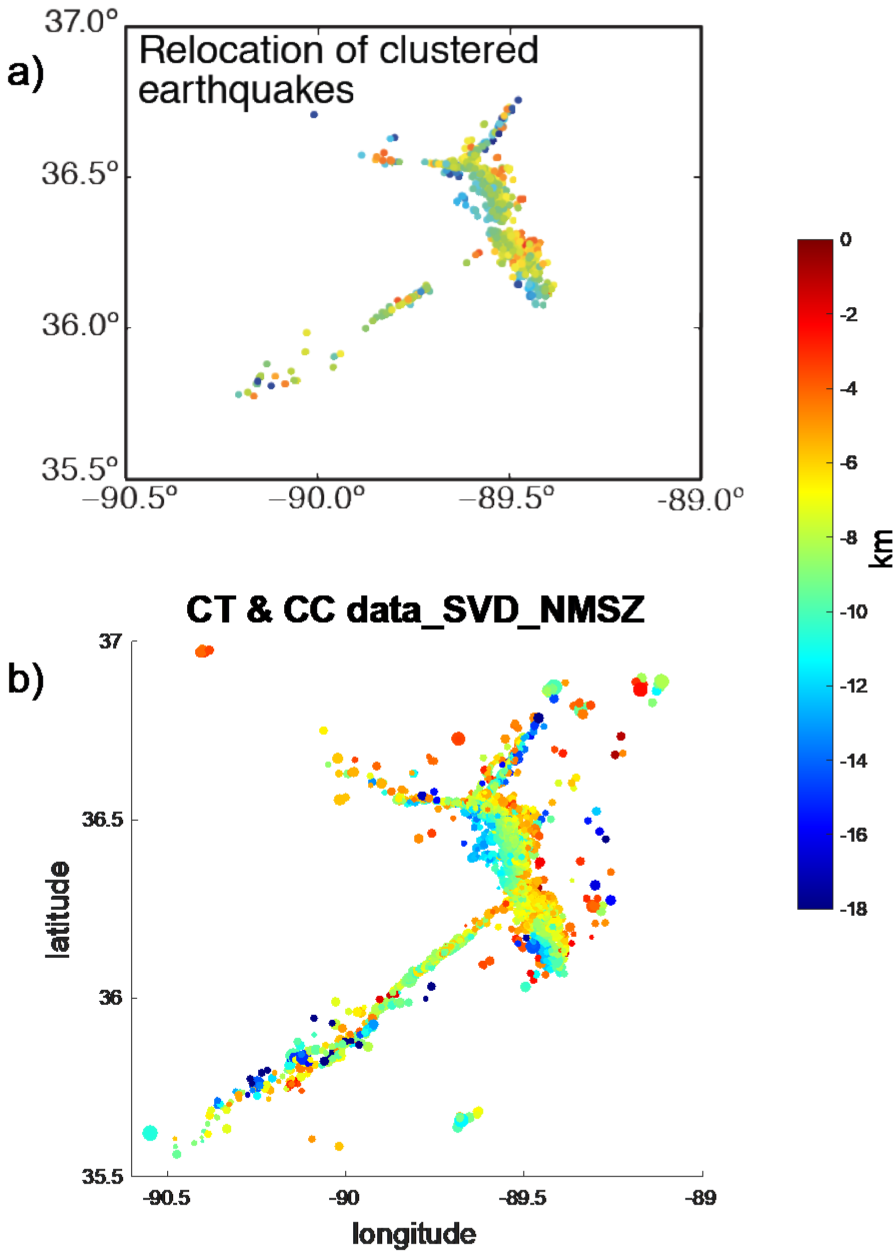

Figure S11. A comparison between the HypoDD results obtained by Dunn et al. (2010) a) and our results b). The availability of a larger dataset has sharpened the fault structure in the NMSZ here.

TABLE S1. WEIGHTING VALUES FOR INPUT DATA				
Iteration	CC P wave weight	CC S wave weight	CT P wave weight	CT S wave weight

1-2	0.01	0.008	1	0.8
3-5	1	0.8	1	0.8
5-8	1	0.5	0.2	0.1

TABLE S2. RELOCATION PARAMETERS AND RESULTS

Cluster	Event # before relocation	Event # after relocation	CND	Damping	RMS CT (ms)	RMS CC (ms)
1	115	111	53	40	42	13
2	218	209	59	45	45	14
3	1251	1192	81	100	39	13
4	1421	1156	79	100	32	7
5	286	286	56	50	33	10
6	357	335	61	55	32	10
7	321	306	69	55	44	9
8	865	839	70	90	39	9

Table S3. PAPAREMERTS of MODELED FAULT PLANES

Part name	Group #	Fault ID	Strike range	Dip range	X mean value	Y mean value	Z mean value	Strike mean value	Dip mean value	Length mean value	Width mean value	Lambda 3 mean value	# of modeled planes
Northern	1	1	60~100	30~60	15.5	6.2	-6.9	73	46	12.5	3.0	0.6	93
		2		75~90	14.7	6.9	-6.0	83	85	11.9	4.0	0.7	140
		3	195~210	75~90	13.5	5.7	-6.2	204	85	4.9	2.1	0.8	35
		4	250~275	0~30	9.0	8.8	-5.2	266	23	5.9	2.1	0.1	35
		5		75~90	11.8	7.8	-5.7	262	86	6.8	2.6	0.4	119
	2	6	10~40	45~75	32.9	5.5	-7.8	30	61	11.2	3.9	0.8	57
		7	80~125	30~60	34.6	4.6	-7.5	102	43	6.7	3.7	0.9	172
		8		75~90	32.2	3.7	-8.1	96	86	11.4	4.0	0.9	242
		9	265~285	75~90	32.5	3.5	-8.1	276	87	9.0	3.4	0.7	105
	3	10	30~50	75~90	41.8	15.8	-9.3	34	83	18.0	5.1	0.9	288
		11	135~155	60~90	42.6	23.6	-5.1	144	73	4.5	2.0	1.1	124
		12	200~230	70~80	47.8	25.7	-8.6	219	75	14.7	2.7	0.4	56
		13		80~90	38.5	11.1	-8.2	212	87	17.9	4.6	0.9	93

		14	240~260	75~90	51.4	32.7	-8.2	249	86	6.5	2.3	0.3	110
RF	1	15	40~70	60~90	38.2	1.4	-8.4	55	77	8.2	2.7	0.8	153
		16	95~125	0~30	41.3	-3.3	-7.4	110	18	14.8	4.7	0.8	102
		17		30~60	40.9	-1.1	-7.5	111	43	8.2	4.4	0.8	82
		18	140~230	15~45	41.0	-4.4	-8.4	172	31	15.8	5.8	0.9	1513
	2	19	100~135	0~30	47.2	-20.8	-6.3	119	18	12.2	6.1	1.0	215
		20	135~165	30~60	46.2	-20.3	-7.5	150	44	14.7	6.0	0.9	312
		21	165~205	15~45	43.9	-18.1	-7.9	185	30	13.5	5.5	0.9	464
		22	290~330	15~45	44.6	-22.7	-7.3	311	29	13.1	4.9	0.9	190
	3	23	20~65	30~75	48.9	-24.6	-6.9	44	52	8.2	4.2	0.8	207
		24	100~170	30~60	49.9	-26.8	-8.3	148	45	15.8	6.2	1.0	682
		25	295~335	15~45	46.6	-25.4	-6.5	314	26	9.7	4.8	0.9	154
AF	1	26	40~70	75~90	22.1	-35.4	-8.1	52	84	21.2	3.9	0.9	296
	2	27	10~90	20~40	-7.4	-61.0	-5.2	72	31	14.8	3.6	0.5	129
		28		50~65	-5.5	-57.8	-7.7	50	57	10.8	2.7	0.5	218
		29		70~90	-8.4	-59.6	-8.6	49	82	13.8	4.0	0.7	547
		30	210~270	75~90	-12.0	-61.3	-12.1	239	85	16.7	4.4	0.6	681
		31	340~350	60~90	-47.8	-78.2	-10.4	344	78	1.4	0.4	0.2	151

Table S1. Weighting values for input data.

Table S2. Relocation parameters and results.

Table S3. Parameters of modeled fault planes.

References:

Dunn, M., Horton, S., DeShon, H., & Powell, C. (2010). High-resolution earthquake relocation in the New Madrid seismic zone. *Seismological Research Letters*, *81*(2), 406-413.